

Phytoplankton growth and stoichiometry under multiple nutrient limitation

Christopher A. Klausmeier¹ and Elena Litchman

School of Biology, Georgia Institute of Technology, 310 Ferst Drive, Atlanta, Georgia 30332-0230

Simon A. Levin

Department of Ecology and Evolutionary Biology, Princeton University, Princeton, New Jersey 08544

Abstract

Phytoplankton growth and stoichiometry depend on the availability of multiple nutrients. We use a mathematical model of phytoplankton with flexible stoichiometry to explain patterns of phytoplankton composition in chemostat experiments and nutrient drawdown dynamics that are found in the field. Exponential growth and equilibrium represent two distinct phases, each amenable to mathematical analysis. In a chemostat at a fixed dilution (growth) rate, phytoplankton stoichiometry matches the nutrient supply stoichiometry over a wide range at low growth rates and over a narrow range at high growth rates. In a chemostat with a fixed nutrient supply stoichiometry, phytoplankton stoichiometry varies with dilution rate nonlinearly, between the supply stoichiometry at low dilution rates and a species-specific optimal ratio at high dilution rates. The flexible-stoichiometry model we study predicts low equilibrium concentrations of two nutrients over a wide range of supply ratios, contrary to the predictions of a traditional fixed-stoichiometry model. The model is in quantitative agreement with experimental data, except at extreme nutrient supply ratios, which require a negative feedback from quota to uptake to fit the data. Our analysis points to the importance of better understanding the regulation of uptake rates in determining phytoplankton stoichiometry and incorporating this knowledge into phytoplankton models.

Phytoplankton require multiple nutrients for growth. Knowledge of how multiple nutrients interact to limit growth is essential to understanding the causes of variation in phytoplankton stoichiometry (Rhee 1978; Goldman et al. 1979), the identity of the nutrient(s) limiting biomass and primary production (Smith 1982), and the effect of resource competition on community structure (Tilman 1982). Of particular interest are nitrogen (N) and phosphorus (P), two macronutrients that are commonly thought to limit phytoplankton (Smith 1982; Downing 1997).

Classic chemostat experiments under multiple-nutrient-limited growth conditions were performed in the 1970s and 1980s (Sterner and Elser 2002). Rhee (1978) grew *Scenedesmus* sp. at a fixed dilution rate with the N:P ratio in the input medium varying from 5 to 80 (by atoms, as throughout this paper). He found that phytoplankton N:P stoichiometry matched the input ratio and that residual nutrients were undetectable. Sterner and Elser (2002) interpreted this as a complete absence of homeostasis over the range of input ratio studies. Other researchers (Goldman et al. 1979; Healey and Hendzel 1979; Ahlgren 1985) fixed the N:P input ratio but controlled the equilibrium growth rate by varying the dilution rate of the chemostat. These studies show that phytoplankton stoichiometry is most variable at low growth rates, with N:P varying from 5 to 100 and carbon (C):P

varying from 60 to 1,200, and that phytoplankton tend to match the input ratio at low growth rates. As the growth rate approaches the maximum growth rate, phytoplankton stoichiometries under N- or P-limitation converge to intermediate values. Some researchers (Goldman et al. 1979) consider these values the Redfield ratios (Redfield 1958; Redfield et al. 1963), but a closer inspection of the data shows that the ratios at the maximum growth rate are species-specific. There is currently no theoretical explanation for the results of either of these types of experiments.

Three elements of a theory of multiple-nutrient-limited growth have been proposed and are well supported experimentally. (1) The relationship between external nutrient concentration and uptake rate often fits Michaelis–Menten kinetics (Turpin 1988). (2) The relationship between the internal concentration (cell quota) of a single limiting nutrient and growth rate is also saturating, with a minimum quota below which growth is zero (Caperon 1968; Droop 1968). The model of growth with one limiting nutrient incorporating these two relations has been tested in both constant and fluctuating environments (Grover 1991a,b; Spijkerman and Coesel 1996). Concerning multiple limiting nutrients, (3) Liebig's law of the minimum has been shown to hold: growth depends on the internal concentration of only the most limiting nutrient (Droop 1974; Rhee 1978).

Although these three elements have been accepted for at least 20 yr, only recently have they been integrated into a mathematical model of multiple nutrient limitation (Legović and Cruzado 1997). Here, we further analyze this model at equilibrium and during exponential growth and compare model predictions to the classic experiments reviewed above. Our goals are the following: (1) to understand the experimental results on the determinants of phytoplankton stoichiometry described above, (2) to explain the patterns of nutrient drawdown found in the field, and (3) to highlight some

¹ Corresponding author (christopher.klausmeier@biology.gatech.edu).

Acknowledgments

We thank T. Daufresne, P. Falkowski, J. Grover, and two anonymous reviewers for comments and discussion. The authors gratefully acknowledge support from the Andrew W. Mellon Foundation (to S.A.L.) and the National Science Foundation awards DEB-0083566 (to S.A.L.), CHE-9810248 (to F. Morel), and OCE-0084032 (to P. Falkowski).

Table 1. Parameter used in numerical solutions unless otherwise noted. Based on Rhee (1974, 1978), with P uptake parameters set within the observed range so that the optimal uptake assumption is met.

Parameter	Meaning (units)	Value
a	Chemostat dilution rate (day^{-1})	0.59
$R_{\text{in}, P}$	Input phosphorus concentration ($\mu\text{mol P L}^{-1}$)	3
$R_{\text{in}, N}$	Input nitrogen concentration ($\mu\text{mol N L}^{-1}$)	15–240
$V_{\text{max}, P}$	Maximum phosphorus uptake rate ($10^{-9} \mu\text{mol P cell}^{-1} \text{day}^{-1}$)	12.3
$V_{\text{max}, N}$	Maximum nitrogen uptake rate ($10^{-9} \mu\text{mol N cell}^{-1} \text{day}^{-1}$)	341
K_P	Phosphorus half-saturation constant ($\mu\text{mol P L}^{-1}$)	0.2
K_N	Nitrogen half-saturation constant ($\mu\text{mol N L}^{-1}$)	5.6
μ_∞	Growth rate at infinite quota (day^{-1})	1.35
m	Mortality rate (day^{-1})	a
$Q_{\text{min}, P}$	Minimum phosphorus quota ($10^{-9} \mu\text{mol P cell}^{-1}$)	1.64
$Q_{\text{min}, N}$	Minimum nitrogen quota ($10^{-9} \mu\text{mol N cell}^{-1}$)	45.4
$Q_{\text{min}, N}/Q_{\text{min}, P}$	Optimal N:P ratio ($\text{mol N} (\text{mol P})^{-1}$)	27.7

critical gaps in our knowledge of multiple-nutrient-limited growth that warrant further empirical and theoretical work.

The model

The model follows phytoplankton and two inorganic nutrients, R_1 and R_2 . Phytoplankton are represented by three variables: cellular quotas (amount of resource per cell) of nutrients 1 and 2 (Q_1 and Q_2) and biomass (B). Nutrients are supplied as in a chemostat, with supply rate a and input concentrations $R_{\text{in},1}$ and $R_{\text{in},2}$. Nutrient uptake depends on inorganic nutrient concentrations but not internal stores. We assume Michaelis–Menten functional forms, $f_i(R_i) = V_{\text{max},i}R_i/(R_i + K_i)$. Quotas increase from nutrient uptake and decrease from growth due to dilution. We assume single-nutrient-limited growth follows Droop's formulation (Droop 1968), $\mu_\infty(1 - Q_{\text{min},i}/Q_i)$, where μ_∞ is the growth rate at infinite quota and $Q_{\text{min},i}$ is the minimum quota of nutrient i at which growth ceases. Multiple-nutrient-limited growth is modeled by the minimum of the functions describing single-nutrient-limited growth, encoding Liebig's law of the minimum. For simplicity, we assume that both nutrients have the same μ_∞ (but see Terry 1985). Biomass increases due to growth and decreases from density-independent mortality at rate $m \geq a$. Together, these assumptions result in the following model:

$$\begin{aligned}
 \frac{dR_1}{dt} &= a(R_{\text{in},1} - R_1) - f_1(R_1)B \\
 \frac{dR_2}{dt} &= a(R_{\text{in},2} - R_2) - f_2(R_2)B \\
 \frac{dQ_1}{dt} &= f_1(R_1) - \mu_\infty \min\left(1 - \frac{Q_{\text{min},1}}{Q_1}, 1 - \frac{Q_{\text{min},2}}{Q_2}\right)Q_1 \\
 \frac{dQ_2}{dt} &= f_2(R_2) - \mu_\infty \min\left(1 - \frac{Q_{\text{min},1}}{Q_1}, 1 - \frac{Q_{\text{min},2}}{Q_2}\right)Q_2 \\
 \frac{dB}{dt} &= \mu_\infty \min\left(1 - \frac{Q_{\text{min},1}}{Q_1}, 1 - \frac{Q_{\text{min},2}}{Q_2}\right)B - mB \quad (1)
 \end{aligned}$$

This model, with the further assumption that $m = a$, was studied by Legović and Cruzado (1997).

It is well known that phytoplankton have some control over their maximum nutrient uptake rates (Rhee 1974, 1978). Therefore, a further assumption we will make at times is the optimal uptake assumption that phytoplankton take up nutrients in an optimal ratio when nutrients are abundant. Mathematically, this means $V_{\text{max},1}/V_{\text{max},2} = Q_{\text{min},1}/Q_{\text{min},2}$. If the minimum quotas represent the functional pools of these nutrients, then this assumption means that when nutrient levels are high, phytoplankton consume nutrients in the ratio required to make new biomass. We note in our analysis below when we make this additional assumption.

Numerical solution

To illustrate the dynamics of growth, we first present numerical solutions of model 1 using parameters based on P- and N-limited growth of the chlorophyte *Scenedesmus* sp. studied by Rhee (1974, 1978) (Table 1). When referring to actual nutrients, we replace numbered subscripts with P and N. These parameters were fixed to meet the optimal uptake assumption. Figures 1, 2 show the dynamics under P- and N-limitation. Both runs start growth with a small inoculum of cells devoid of stored nutrients and nutrient levels at their input concentrations. In both cases, biomass grows sigmoidally over time, approaching a stable equilibrium (Figs. 1A, 2A). Nutrients are drawn down in the same fixed ratio until one nutrient reaches low concentration (Figs. 1B, 2B). Phytoplankton N:P stoichiometry (measured as Q_N/Q_P) shows two distinct phases (Figs. 1C, 2C). During the exponential growth phase, phytoplankton N:P is constant and similar in both runs. As equilibrium is approached, phytoplankton N:P diverges toward a higher value under P-limitation (Fig. 1C) and toward a lower value under N-limitation (Fig. 2C). In these particular cases, the equilibrium N:P closely resembles the input N:P, $R_{\text{in},N}/R_{\text{in},P}$. The occurrence of two distinct growth phases suggests a natural division for our model analysis that follows.

Model analysis: Exponential phase

During exponential growth, quotas quickly reach a quasi-equilibrium while nutrients are still abundant (Figs. 1, 2).

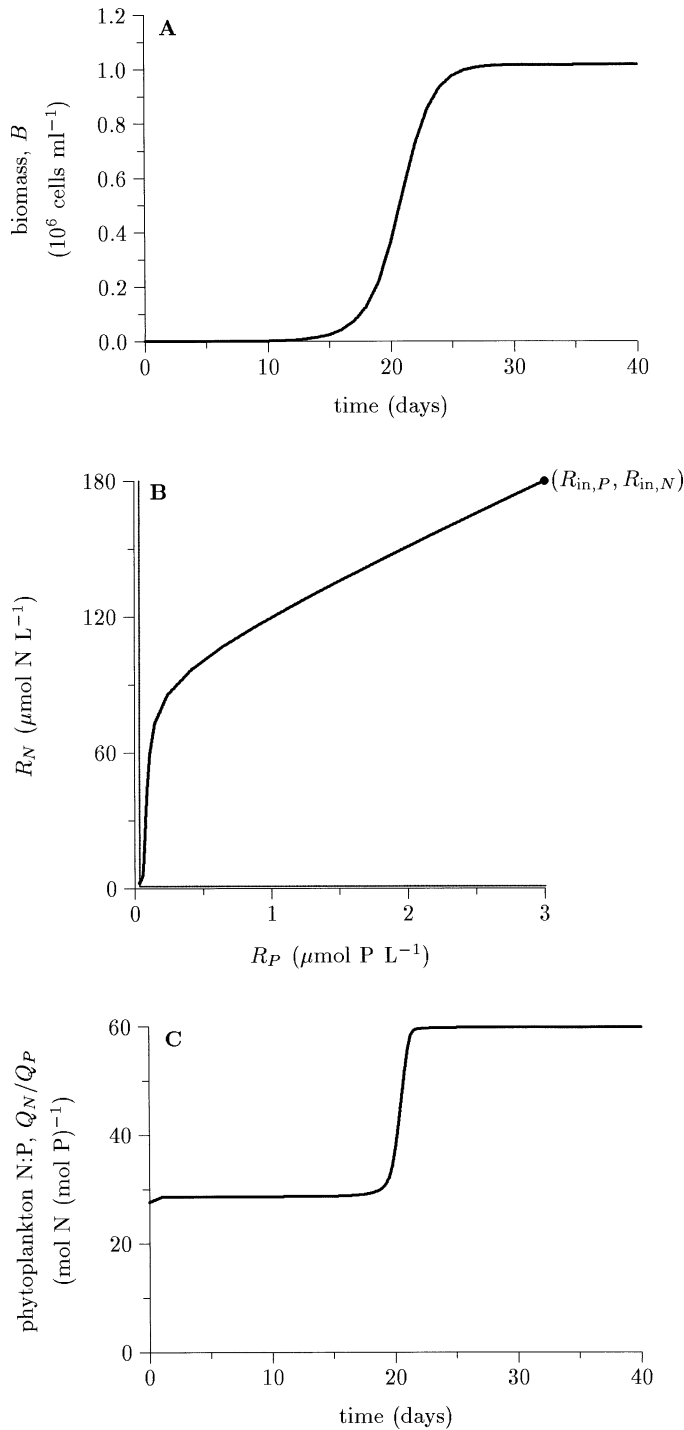


Fig. 1. Numerical solution of model 1 under P-limitation. $R_{in,P} = 3$, $R_{in,N} = 180$; other parameters are given in Table 1. (A) Biomass versus time. (B) Available phosphorus and nitrogen. The right-angle line is the zero net growth isocline (Tilman 1982). (C) Phytoplankton N:P stoichiometry versus time.

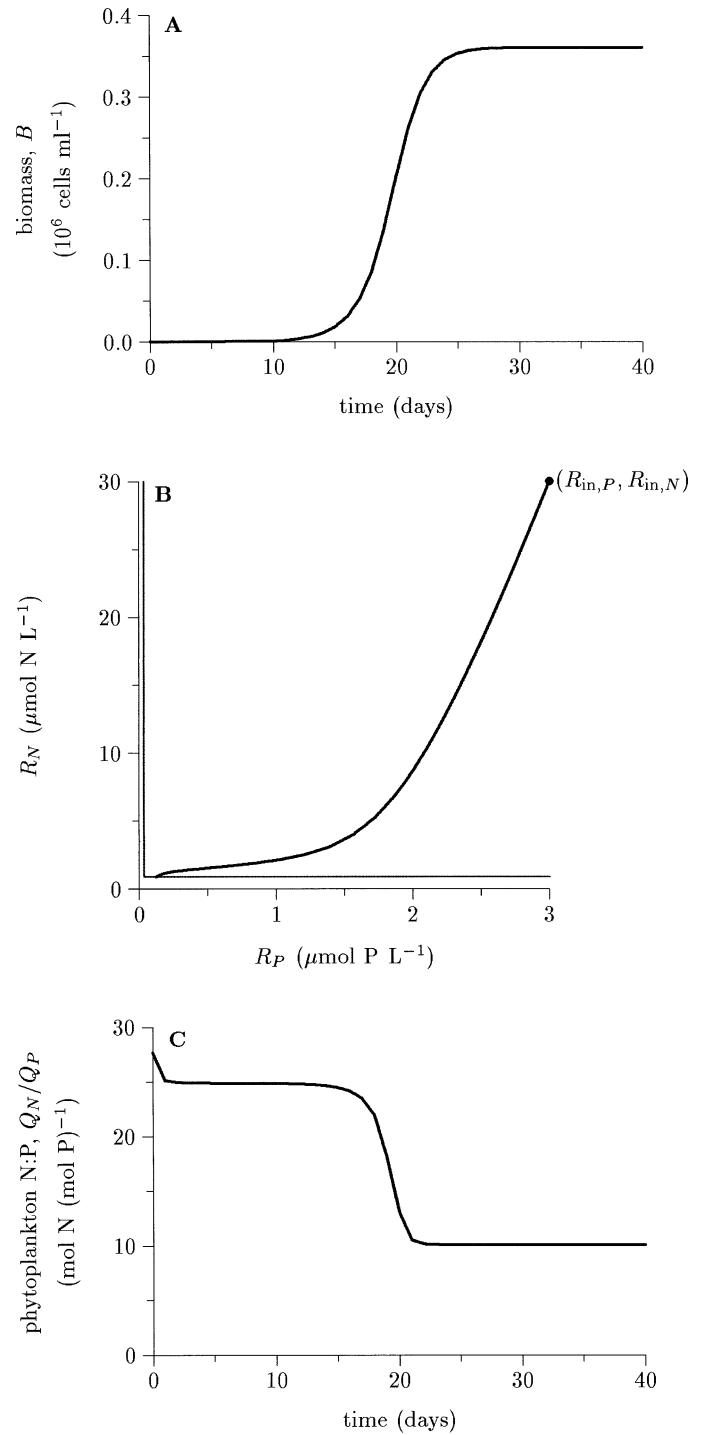


Fig. 2. Numerical solution of model 1 under N-limitation. $R_{in,P} = 3$, $R_{in,N} = 30$; other parameters are given in Table 1. (A–C) As in Fig. 1.

Thus, to approximate the dynamics during exponential growth, we set $R_1 = R_{in,1}$, $R_2 = R_{in,2}$, $dQ_1/dt = 0$, and $dQ_2/dt = 0$ and solve for \tilde{Q}_1 and \tilde{Q}_2 , where tildes denote quasi-equilibrium values. We find

$$\tilde{Q}_{lim} = Q_{min,lim} + \frac{f_{lim}(R_{in,lim})}{\mu_{\infty}} \quad (2)$$

$$\tilde{Q}_{non} = \frac{f_{non}(R_{in,non})}{f_{lim}(R_{in,lim})} \tilde{Q}_{lim} \quad (3)$$

where the subscripts “lim” and “non” denote the limiting and nonlimiting resources, respectively, determined by $Q_{\text{lim}}/Q_{\text{non}} > Q_{\text{min,non}}/Q_{\text{min,lim}}$. Substituting Eq. 2 into dB/dt , we find the realized maximum growth rate to be

$$\mu_{\text{max}} = \frac{\mu_{\infty} f_{\text{lim}}(R_{\text{in,lim}})}{\mu_{\infty} Q_{\text{min,lim}} + f_{\text{lim}}(R_{\text{in,lim}})} \quad (4)$$

The phytoplankton stoichiometry is the same regardless of which nutrient is limiting.

$$\frac{\hat{Q}_1}{\hat{Q}_2} = \frac{f_1(R_{\text{in},1})}{f_2(R_{\text{in},2})} \quad (5)$$

Under the optimal uptake assumption, when nutrients are saturating,

$$\frac{\hat{Q}_1}{\hat{Q}_2} \approx \frac{Q_{\text{min},1}}{Q_{\text{min},2}} \quad (6)$$

Because phytoplankton consume nutrients in the ratio given by Eq. 5, this also corresponds to the consumption vector (sensu Tilman 1982), which is the slope of nutrient draw-down shown in the exponential phase of the numerical solutions (Figs. 1B, 2B). Thus, during exponential growth, phytoplankton “are what they eat” (Sterner and Elser 2002), and if the optimal uptake assumption holds, they “eat what they need.”

Model analysis: Equilibrium phase

To analyze model 1 at equilibrium, we set all time derivatives equal to zero. Because of the minimum term in the growth equation, one nutrient alone usually limits growth. $dB/dt = 0$ implies

$$\hat{Q}_{\text{lim}} = Q_{\text{min,lim}} \frac{\mu_{\infty}}{\mu_{\infty} - m} \quad (7)$$

where hats represent equilibrium values. Setting $dQ_{\text{lim}}/dt = 0$ determines the available pool of the limiting nutrient, which is the phytoplankton’s break-even concentration, R^* ,

$$\begin{aligned} \hat{R}_{\text{lim}} = R_{\text{lim}}^* &= f_{\text{lim}}^{-1} \left(\frac{Q_{\text{min,lim}} m \mu_{\infty}}{\mu_{\infty} - m} \right) \\ &= \frac{Q_{\text{min,lim}} m \mu_{\infty} K_{\text{lim}}}{V_{\text{max,lim}} (\mu_{\infty} - m) - Q_{\text{min,lim}} m \mu_{\infty}} \end{aligned} \quad (8)$$

Biomass is given by setting $dR_{\text{lim}}/dt = 0$,

$$\hat{B} = \frac{a(R_{\text{in,lim}} - R_{\text{lim}}^*)}{\hat{Q}_{\text{lim}} m} = \frac{a(R_{\text{in,lim}} - R_{\text{lim}}^*)(\mu_{\infty} - m)}{Q_{\text{min,lim}} \mu_{\infty} m} \quad (9)$$

The equilibrium quota of the nonlimiting nutrient is

$$\hat{Q}_{\text{non}} = \frac{f_{\text{non}}(\hat{R}_{\text{non}})}{m} \quad (10)$$

which depends on \hat{R}_{non} . The algebraic expressions for equilibrium values of \hat{Q}_{non} and \hat{R}_{non} are unwieldy, but they can easily be determined numerically.

The zero net growth isocline (ZNGI), the set of (R_1, R_2) for which growth ceases, is a right-angle curve made of R_1

$= R_1^*$ when $R_2 \geq R_2^*$ and $R_2 = R_2^*$ when $R_1 \geq R_1^*$, as is typical of essential resources (Tilman 1982). Figures 1B, 2B illustrate the ZNGI close to the axes and show that available nutrient levels are drawn down to lie on the ZNGI at equilibrium. Legović and Cruzado (1997) show that the equilibrium is linearly stable when $m = a$, and we have proven it is stable for any m .

Figure 3 shows the influence of the nutrient supply ratio on phytoplankton stoichiometry, parameterized to match Rhee’s (1978) *Scenedesmus* experiments. Figure 3A,B shows equilibrium N and P quotas, respectively. The model predictions (solid lines) closely match Rhee’s experimental data (points). The model also accurately predicts the equilibrium cell density (data not shown). The N quota is low and independent of the N:P supply ratio when N is limiting, and it increases with increasing N:P supply when P is limiting (Fig. 3A). The P quota is low and independent of the N:P supply ratio when it is limiting, and it increases with decreasing N:P supply when N is limiting (Fig. 3B). Figure 3C shows how the N:P supply ratio affects phytoplankton N:P. For low dilution (growth) rates, phytoplankton stoichiometry matches the nutrient supply ratio over most of the range shown, such as for Rhee’s experiments where $a = 0.59 \text{ d}^{-1}$. However, for higher dilution rates, the curves become sigmoidal, revealing a limit to the flexibility of phytoplankton stoichiometry.

Figure 4 shows the influence of dilution rate on phytoplankton stoichiometry in a chemostat, as in the study by Goldman et al. (1979). Under N- (dotted line) or P-limitation (dashed line), the phytoplankton N:P stoichiometry equals the input ratio at low growth rates (Fig. 4A). This occurs because phytoplankton consume almost all the nutrients that enter the chemostat. This result is exact when $m = a$ as in a perfect chemostat, and it is approximate when $m > a$. At growth rates close to maximal, the phytoplankton stoichiometry approaches $f_N(R_{\text{in,N}})/f_P(R_{\text{in,P}})$; because phytoplankton biomass is low, they have little effect on the nutrient concentrations, and therefore, they match the exponential growth case given by Eq. 5. When phytoplankton are supplied nutrients in their optimal N:P ratio (solid line), they maintain this N:P ratio in their biomass over the range of growth rates, under the optimal uptake assumption.

The effect of dilution rate on the quota of the limiting nutrient is given by Eq. 7, which shows that the quota increases with dilution rate (Fig. 4B, solid line). The effect of dilution rate on the quota of a nonlimiting nutrient is less straightforward, and it depends on the input ratio. When a species is close to colimitation, the quota of the nonlimiting nutrient appears to fit the Droop equation but with a greater quota for a given growth rate than when limiting conditions are examined (Fig. 4B, dot-dashed line). The more the supply ratio deviates from the species optimum ratio, the higher the quota of the nonlimiting nutrient. When the supply ratio is sufficiently different from the species optimum ratio, the slope of the quota-versus-dilution rate curve becomes negative at high dilution rates, and the quota of the nonlimiting nutrient reaches a maximum at an intermediate dilution rate (Fig. 4B, dashed and dotted lines).

We can understand these results heuristically using two approximations. At high mortality rates (m close to μ_{max}),

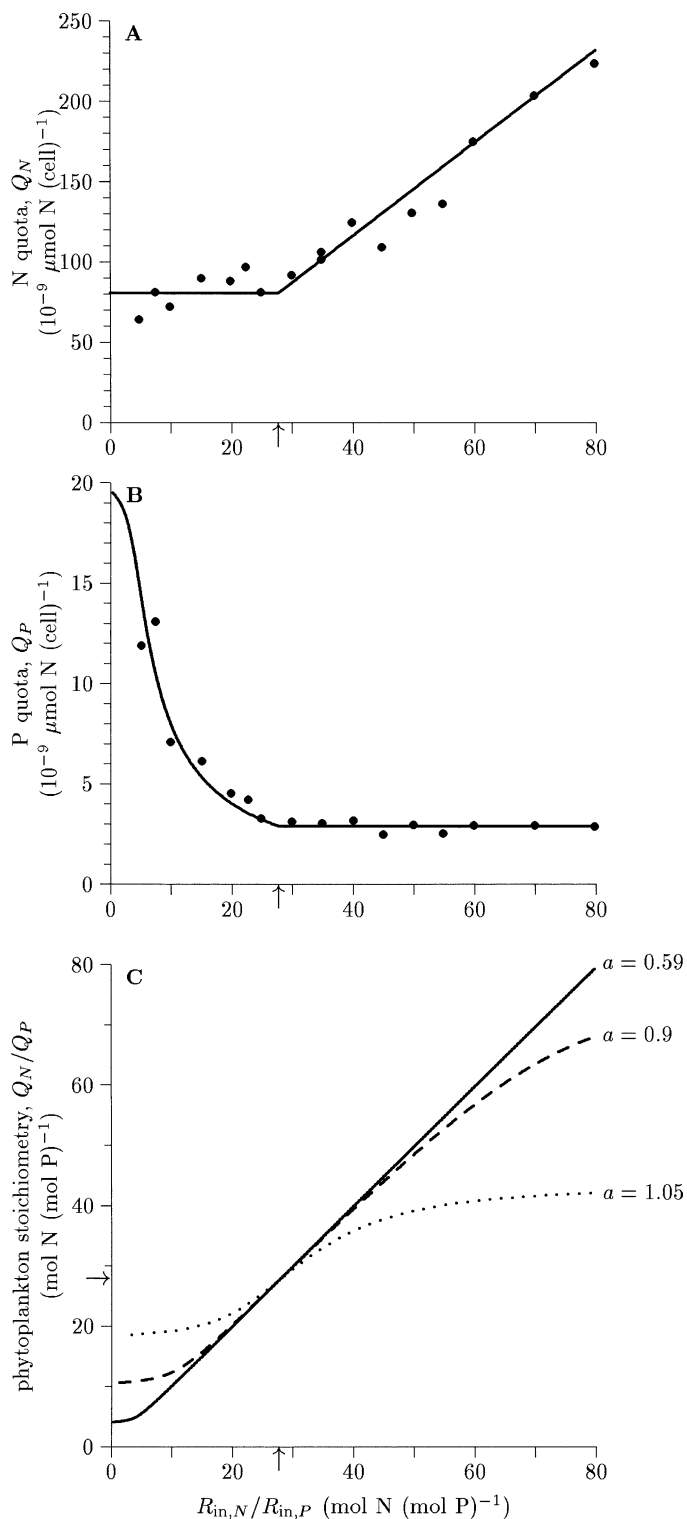


Fig. 3. Equilibrium phytoplankton stoichiometry as a function of nutrient supply stoichiometry. Parameters are given in Table 1. Arrows on the axes show the phytoplankton's optimal N:P ratio, the border between N- and P-limitation. (A) N and (B) P quota with $a = 0.59 \text{ d}^{-1}$. The solid line gives model predictions; the dots are corresponding experimental measurements taken from Rhee (1978). (C) Model predicted phytoplankton N:P under three dilution (growth) rates. The solid line represents Rhee's (1978) experimental setup, with dilution (growth) rate $a = 0.59 \text{ d}^{-1}$. The dashed and dotted lines represent higher dilution rates, $a = 0.9$ and $a = 1.05 \text{ d}^{-1}$, respectively.

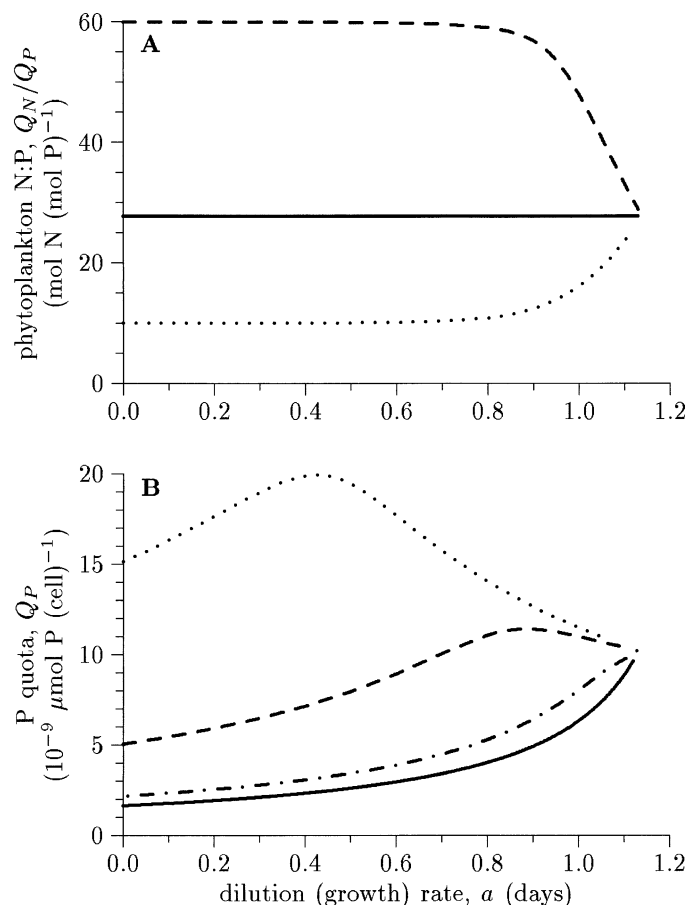


Fig. 4. Equilibrium phytoplankton stoichiometry as a function of dilution (growth) rate. In all cases, $R_{in,P} = 3$, and other parameters are given in Table 1. (A) Phytoplankton N:P. The dashed line represents P-limitation ($R_{in,N}/R_{in,P} = 60$); the solid line represents co-limitation ($R_{in,N}/R_{in,P} = 27.7$); and the dotted line represents N-limitation ($R_{in,N}/R_{in,P} = 10$). (B) Phytoplankton P quota, \hat{Q}_P . The solid line represents P-limitation ($R_{in,N}/R_{in,P} \geq 27.7$); the dot-dashed line represents mild N-limitation ($R_{in,N}/R_{in,P} = 21$); and the dashed and dotted lines represent stronger N-limitation ($R_{in,N}/R_{in,P} = 9$ and 3 , respectively).

the available pool of the nonlimiting nutrient is large, and uptake is approximately maximal. Equation 10 shows that

$$\hat{Q}_{\text{non}} \approx \frac{V_{\text{max,non}}}{m} \quad (11)$$

which explains the negative slope at high dilution rates in the dashed and dotted lines of Fig. 4B. In this case, the quota of the nonlimiting nutrient is uptake-limited. At low mortality rates (m close to zero), the available pool of both nutrients is small ($R_i \approx 0$). In a perfect chemostat ($m = a$), the phytoplankton must contain almost all the nutrients supplied. Then,

$$\hat{Q}_{\text{non}} \approx \frac{R_{in,\text{non}}}{\hat{B}} \approx \frac{R_{in,\text{non}}}{R_{in,\text{lim}}} Q_{\text{min,lim}} \frac{\mu_{\infty}}{\mu_{\infty} - a} \quad (12)$$

Here, the quota of the nonlimiting nutrient increases with dilution rate, as for small a in Fig. 4B. In this case, the quota

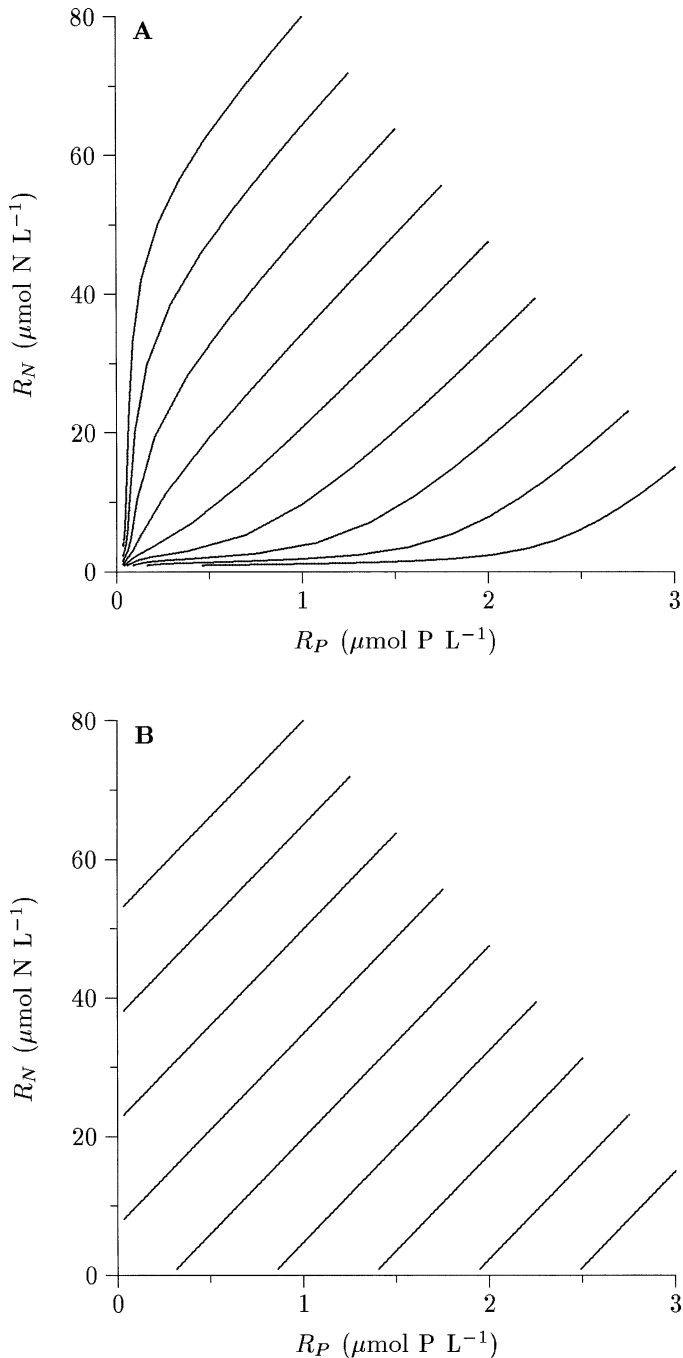


Fig. 5. Nutrient drawdown patterns for a range of nutrient supply ratios. (A) Using model 1 with flexible phytoplankton stoichiometry. Parameters are given in Table 1. (B) Using an analogous model with fixed phytoplankton stoichiometry.

of the nonlimiting nutrient is supply-limited. Note that Eq. 12 is a rescaled version of the Droop expression in Eq. 7. Near colimitation, the supply-limited approximation is valid over the whole range of a ; away from colimitation, the supply-limited approximation is valid for small a , and the uptake-limited approximation is valid for large a .

Figure 5 compares the nutrient drawdown patterns in model 1 and an analogous fixed stoichiometry model (Til-

man 1982). Regardless of the nutrient-limiting growth, phytoplankton reduce both nutrients to low levels in the flexible stoichiometry model 1 (Fig. 5A). In contrast, the fixed stoichiometry model leaves the available concentrations of the nonlimiting nutrient at high concentrations and results in low concentrations of both nutrients only when the supply ratio is close to the optimal ratio (Fig. 5B).

Model extension: Uptake inhibition

Although model 1 correctly predicts the results of Rhee's 1978 chemostat experiments (Fig. 3), it ignores many aspects of nutrient-limited phytoplankton growth. One particularly relevant aspect that is neglected is negative feedback from internal nutrient stores to uptake rates. This has been demonstrated for many species (e.g., Rhee 1974, 1978; Morel 1987). Commonly, this inhibition is summarized by treating the maximum uptake rate of a nutrient as a decreasing function of its quota. DiToro (1980) has shown that for single-nutrient-limited growth, models without uptake inhibition can grossly overestimate the maximum quota of a limiting nutrient.

To test whether our model of multiple-nutrient limitation also overestimates the flexibility of phytoplankton stoichiometry, we compared model predictions to three other of Rhee's experiments with *Scenedesmus* sp., where he measured cellular stoichiometry with extreme supply ratios (Rhee 1974). Outside the range of N:P supply ratios shown in Fig. 3, our model consistently overpredicts the quota of the nonlimiting nutrient (Table 2). Numerical solution of a variant of model 1 with maximum uptake rates dependent on quotas, using the functions and parameters given by Gotham and Rhee (1981a,b), does a better job. This modified model also accurately predicts the data shown in Fig. 3, except for underpredicting Q_N under severe P-limitation (data not shown). However, a different parameterization of the $V_{\max,N}(Q_N)$ function at high Q_N fixes this problem (data not shown).

Discussion

Model predictions—Model 1 makes a number of predictions about the determinants of phytoplankton growth and stoichiometry and nutrient drawdown patterns. We compare them with field observations and laboratory experiments.

First, the temporal dynamics of nutrient drawdown during growth show two phases (Figs. 1, 2, 5A). At high nutrient levels, nutrients are consumed in a fixed ratio. Under the optimal uptake assumption, the consumption ratio and the phytoplankton stoichiometry are approximately optimal. After one nutrient is depleted and limits growth, uptake of the nonlimiting nutrient continues, and phytoplankton stoichiometry deviates from optimal. Redfield et al. (1963) report such drawdown patterns from the Long Island Sound. Because phytoplankton vary in their optimal N:P ratios, $Q_{\min,N}/Q_{\min,P}$ (Rhee and Gotham 1980; Hecky and Kilham 1988; Andersen 1997), we expect the initial drawdown ratio to be species-specific, as was demonstrated in the Southern Ocean by Arrigo et al. (1999).

Table 2. Comparison of Rhee (1974) experiments with model 1 and a modified model that includes inhibition of nutrient uptake, parameterized according to Gotham and Rhee (1981a, b), so that $V_{\max} = (v_{\max} K_{\text{inh}} - c(Q - Q_{\text{min}}))/(Q - Q_{\text{min}} + K_{\text{inh}})$. For N, $v_{\max} = 1,320 \times 10^{-9} \mu\text{mol N cell}^{-1} \text{d}^{-1}$, $c = 0$, and $K_{\text{inh}} = 10.99 \times 10^{-9} \mu\text{mol N cell}^{-1}$. For P, $v_{\max} = 93.17 \times 10^{-9} \mu\text{mol P cell}^{-1} \text{d}^{-1}$, $c = 102.8 \times 10^{-9} \mu\text{mol P cell}^{-1} \text{d}^{-1}$, and $K_{\text{inh}} = 14.85 \times 10^{-9} \mu\text{mol P cell}^{-1}$. $R_{\text{in},N}$ and $R_{\text{in},P}$ are given in units of $10^{-9} \mu\text{mol L}^{-1}$, a in units of day^{-1} , and Q 's in units of $10^{-9} \mu\text{mol cell}^{-1}$.

Limitation	$R_{\text{in},N}$	$R_{\text{in},P}$	a	Observed		Model 1		Inhibition model	
				Q_N	Q_P	Q_N	Q_P	Q_N	Q_P
N	10.0	10.0	0.63	74.73	10.41	85.1	19.0	85.1	12.9
N	22.1	10.0	0.68	86.33	11.7	91.5	17.5	91.5	12.8
P	2,000	1.06	0.68	215.0	3.07	500	3.3	164	3.3

Second, the model predicts low nutrient levels of both limiting and nonlimiting nutrients at equilibrium (Fig. 5A). This contrasts with the predictions of an analogous fixed-stoichiometry model (Tilman 1982), which shows simultaneous depletion of both nutrients only when the supply ratio matches the optimal ratio (Fig. 5B). Dissolved organic and inorganic N and P were undetectable in Rhee's experiments regardless of which nutrient was limiting (1978). Simultaneous depletion of N and P to low levels is common in lakes and the ocean, so we suggest that analytical and simulation models incorporate flexible phytoplankton stoichiometry if they seek to explain available nutrient concentrations and resource competition.

The third and fourth predictions concern how the dilution (growth) rate and the nutrient supply ratio interact to determine phytoplankton stoichiometry in chemostat cultures. At low dilution (growth) rates, phytoplankton stoichiometry matches the nutrient supply ratio (Fig. 3C). At low dilution rates, available nutrients are quite scarce, and phytoplankton consume almost all the nutrients that are supplied, therefore matching the input ratio. In Sterner and Elser's terms (2002), they "are what they eat," and furthermore, they "eat what they are served." At high dilution rates, phytoplankton stoichiometry is less variable (Fig. 3C). This occurs because the phytoplankton in a chemostat are perpetually growing exponentially, and when the dilution rate is high, nutrient levels are also high. In this case, they begin to match their optimal ratio as in the exponential growth case, given the optimal uptake assumption. Cells "eat what they need." Figure 3 was parameterized using the species parameters from Rhee's classic experiments (1978). The solid line in Fig. 3C, which represents the same experimental dilution rate as in Rhee, gives results identical to those in his experiments: the phytoplankton are perfectly flexible over the range of N:P inputs examined. However, as the other lines show, if Rhee had run his experiments at a higher dilution rate, the phytoplankton stoichiometry would appear less variable.

The effect of varying dilution rate for a fixed N:P supply ratio was investigated experimentally (Goldman et al. 1979; Healey and Hendzel 1979; Ahlgren 1985). Figure 4 corresponds to this type of experiment and qualitatively matches the experimental findings. At low growth rates, phytoplankton N:P stoichiometry matches the supply ratio, while at high growth rates, phytoplankton stoichiometry approaches the optimal ratio under the optimal uptake assumption (Fig. 4A). Goldman et al. (1979) report the same pattern empirically (reprinted as fig. 3.3A in Sterner and Elser 2002).

Again, because the optimal N:P ratio is species-specific (Rhee and Gotham 1980; Hecky and Kilham 1988; Andersen 1997), the phytoplankton N:P ratios at high growth rates do not reflect a universal Redfield ratio, contrary to Goldman et al. (1979). The predicted relationship between growth rate and phytoplankton N:P stoichiometry is not linear but can be constant over a range of low growth rates (Fig. 4A).

The effect of dilution rate on the quota of the nonlimiting nutrient is more complicated. Near colimitation, Q_{non} increases with dilution rate over the range of possible dilution rates (Fig. 4B). The relationship between dilution rate and Q_{non} approximately follows a Droop relationship, except with an apparent $Q_{\text{min,non}} = (R_{\text{in,non}}/R_{\text{in,lim}})Q_{\text{min,lim}}$ (Eq. 12). This explains why the Droop model can often fit quota data for both limiting and nonlimiting nutrients (Droop 1974). However, far from colimitation, our model predicts that Q_{non} increases at low dilution rates (perhaps only slightly) and decreases at high dilution rates. This decrease at high dilution rates occurs when uptake of the nonlimiting nutrient is saturated. This may explain why the C:P ratio of *Thalassiosira pseudonana* increased with growth rate under N-limitation (Goldman et al. 1979).

Overall, the agreement between the model predictions and field studies and laboratory experiments suggests that model 1 captures many essential features of multiple-nutrient-limited growth. We agree with Legović and Cruzado (1997), who first analyzed this model, that it would be a useful subcomponent of more complex ecosystem simulations. In the case of *Scenedesmus* that we examined quantitatively, including the inhibition of nutrient uptake by internal stores improved the model predictions only at extreme nutrient supply ratios. Grover (1991a) also noted that inhibition of nutrient uptake did not improve the ability of a single-nutrient Droop model to predict competitive outcome in non-equilibrium experiments.

Our analysis points out one crucial but still poorly understood physiological process: the regulation of uptake rates. These rates are important because they alone determine phytoplankton stoichiometry during exponential growth at high nutrient levels (Eq. 5). When we make the optimal uptake assumption, we assume phytoplankton consume nutrients in the ratio they require when nutrients are saturating. This makes sense for species that typically bloom in response to high nutrients, but perhaps other species that favor equilibrium conditions are preadapted to consume nutrients at the optimal ratio at low levels. The empirical validity of our optimal uptake assumption is not clear. Our model treats

maximum uptake rates as fixed constants, but they are known to vary widely with growth conditions (Rhee 1974, 1978). Biologically, uptake rates can be rapidly altered by shutting down uptake proteins, exuding alkaline phosphatases, or, more slowly, by changing the rates of uptake protein synthesis and degradation. Existing experimental (Gotham and Rhee 1981*a,b*) and theoretical (Andersen 1997) studies that include regulation of maximal uptake rates assume that they depend only on the internal stores of the same nutrient and that this feedback is rapid. We suspect that the regulation of uptake may be more complicated, varying on different timescales and depending on internal stores of both limiting and nonlimiting nutrients. Models that include a more mechanistic approach to nutrient uptake regulation will further our understanding of phytoplankton stoichiometry.

References

- AHLGREN, G. 1985. Growth of *Oscillatoria agardhii* in chemostat culture 3. Simultaneous limitation of nitrogen and phosphorus. *Br. Phycol. J.* **20**: 249–261.
- ANDERSEN, T. 1997. Pelagic nutrient cycles: Herbivores as sources and sinks. Springer.
- ARRIGO, K. R., D. H. ROBINSON, D. L. WORTHEN, R. B. DUNBAR, G. R. DiTULLIO, M. VAN WOERT, AND M. P. LIZOTTE. 1999. Phytoplankton community structure and the drawdown of nutrients and CO₂ in the Southern Ocean. *Science* **283**: 365–367.
- CAPERON, J. 1968. Population growth response of *Isochrysis galbana* to nitrate variation at limiting concentrations. *Ecology* **49**: 866–872.
- DiTORO, D. M. 1980. Applicability of cellular equilibrium and Monod theory to phytoplankton growth kinetics. *Ecol. Model.* **8**: 201–218.
- DOWNING, J. A. 1997. Marine nitrogen:phosphorus stoichiometry and the global N:P cycle. *Biogeochemistry* **37**: 237–252.
- DROOP, M. R. 1968. Vitamin B₁₂ and marine ecology. 4. The kinetics of uptake, growth and inhibition of *Monochrysis lutheri*. *J. Mar. Biol. Assoc. UK* **48**: 689–733.
- . 1974. The nutrient status of algal cells in continuous culture. *J. Mar. Biol. Assoc. UK* **54**: 825–855.
- GOLDMAN, J. C., J. J. MCCARTHY, AND D. G. PEAVEY. 1979. Growth rate influence on the chemical composition of phytoplankton in oceanic waters. *Nature* **279**: 210–215.
- GOTHAM, I. J., AND G.-Y. RHEE. 1981*a*. Comparative kinetic studies of phosphate-limited growth and phosphate uptake in phytoplankton in continuous culture. *J. Phycol.* **17**: 257–265.
- , AND ———. 1981*b*. Comparative kinetic studies of nitrate-limited growth and nitrate uptake in phytoplankton in continuous culture. *J. Phycol.* **17**: 309–314.
- GROVER, J. P. 1991*a*. Non-steady state dynamics of algal population growth: Experiments with two Chlorophytes. *J. Phycol.* **27**: 70–79.
- . 1991*b*. Resource competition among microalgae in variable environments: Experimental tests of alternative models. *Oikos* **62**: 231–243.
- HEALEY, F. P., AND L. L. HENDZEL. 1979. Indicators of phosphorus and nitrogen deficiency in five algae in culture. *J. Fish. Res. Board Can.* **36**: 1364–1369.
- HECKY, R. E., AND P. KILHAM. 1988. Nutrient limitation of phytoplankton in freshwater and marine environments: A review of recent evidence on the effects of enrichment. *Limnol. Oceanogr.* **33**: 796–822.
- LEGOVIĆ, T., AND A. CRUZADO. 1997. A model of phytoplankton growth on multiple nutrients based on the Michaelis–Menten–Monod uptake, Droop's growth and Liebig's law. *Ecol. Model.* **99**: 19–31.
- MOREL, F. M. M. 1987. Kinetics of nutrient uptake and growth in phytoplankton. *J. Phycol.* **23**: 137–150.
- REDFIELD, A. C. 1958. The biological control of chemical factors in the environment. *Am. Sci.* **46**: 205–221.
- , B. H. KETCHUM, AND F. A. RICHARDS. 1963. The influence of organisms on the composition of sea-water, p. 26–77. *In* M. Hill [ed.], *The sea*. Interscience.
- RHEE, G.-Y. 1974. Phosphate uptake under nitrate limitation by *Scenedesmus* sp. and its ecological implications. *J. Phycol.* **10**: 470–475.
- . 1978. Effects of N:P atomic ratios and nitrate limitation on algal growth, cell composition, and nitrate uptake. *Limnol. Oceanogr.* **23**: 10–25.
- , AND I. J. GOTHAM. 1980. Optimum N:P ratios and coexistence of planktonic algae. *J. Phycol.* **16**: 486–489.
- SMITH, V. H. 1982. The nitrogen and phosphorus dependence of algal biomass in lakes: An empirical and theoretical analysis. *Limnol. Oceanogr.* **27**: 1101–1112.
- SPIJKERMAN, E., AND P. F. M. COESEL. 1996. Competition for phosphorus between planktonic desmid species in continuous-flow culture. *J. Phycol.* **32**: 939–948.
- STERNER, R. W., AND J. J. ELSER. 2002. *Ecological stoichiometry: The biology of elements from molecules to the biosphere*. Princeton Univ. Press.
- TERRY, K. L. 1985. Growth rate variation of the N:P requirement ratio of phytoplankton. *J. Phycol.* **21**: 323–329.
- TILMAN, D. 1982. *Resource competition and community structure*. Princeton Univ. Press.
- TURPIN, D. H. 1988. Physiological mechanisms in phytoplankton resource competition, p. 316–368. *In* C. D. Sandgren [ed.], *Growth and reproductive strategies of freshwater phytoplankton*. Cambridge Univ. Press.

Received: 28 February 2003
 Amended: 10 November 2003
 Accepted: 17 November 2003